

UKAEA-CCFE-PR(20)64

D. Iglesias, W. Arter, I. Balboa, P. Bunting, C. Challis,
J.W. Coenen, Y. Corre, S. Esquembri, S. Jachmich,
K. Krieger, G.F. Matthews, R.A. Pittsh, V. Riccardo,
M.L. Richiusa, M. Porton, F. Rimini, S. Silburn, V.K.
Thompson, R. Otin, D. Valcarcel, L. Vitton-Mea, Z.
Vizvary, J. Williams, JET contributors

Advances in predictive thermo- mechanical modelling for the JET divertor experimental interpretation, improved protection, and reliable operation

Enquiries about copyright and reproduction should in the first instance be addressed to the UKAEA Publications Officer, Culham Science Centre, Building K1/O/83 Abingdon, Oxfordshire, OX14 3DB, UK. The United Kingdom Atomic Energy Authority is the copyright holder.

The contents of this document and all other UKAEA Preprints, Reports and Conference Papers are available to view online free at scientific-publications.ukaea.uk/

Advances in predictive thermo-mechanical modelling for the JET divertor experimental interpretation, improved protection, and reliable operation

D. Iglesias, W. Arter, I. Balboa, P. Bunting, C. Challis, J.W. Coenen, Y. Corre, S. Esquembri, S. Jachmich, K. Krieger, G.F. Matthews, R.A. Pittsh, V. Riccardo, M.L. Richiusa, M. Porton, F. Rimini, S. Silburn, V.K. Thompson, R. Otin, D. Valcarcel, L. Vitton-Mea, Z. Vizvary, J. Williams, JET contributors

Advances in predictive thermo-mechanical modelling for the JET divertor experimental interpretation, improved protection, and reliable operation

**D. Iglesias^a, W. Arter^a, I. Balboa^a, P. Bunting^a, C. Challis^a,
J.W. Coenen^b, Y. Corre^c, S. Esquembri^d, S. Jachmich^{e,f}, K. Krieger^g,
G.F. Matthews^a, R.A. Pitts^h, V. Riccardoⁱ, M.L. Richiusa^a, M. Porton^a,
F. Rimini^a, S. Silburn^a, V.K. Thompson^a, R. Otin^a, D. Valcarcel^a,
L. Vitton-Mea^j, Z. Vizvary^a, J. Williams^a, and JET contributors***

EUROfusion Consortium, JET, Culham Science Centre (CSC), Abingdon, OX14 3DB, UK

^aUKAEA - Culham Centre for Fusion Energy, Abingdon, OX14 3DB, UK

^bForschungszentrum Jülich GmbH, Institut für Energie- und Klimaforschung –

Plasmaphysik, Partner of the Trilateral Euregio Cluster (TEC), 52425 Jülich, Germany

^cCEA, IRFM, Saint-Paul-Lez-Durance, France

^dUPM, Technical University of Madrid, Madrid, Spain

^eEUROfusion PMU, JET, Culham Science Centre, Abingdon, U.K. ^fLPP, Ecole Royale

Militaire/Koninklijke Militaire School, TEC partner, Brussels, Belgium ^gMax-Planck-Institut für Plasmaphysik, Garching, Germany

^hITER Organization, Route de Vinon-sur-Verdon, CS 90 046, 13067 St. Paul Lez Durance Cedex, France

ⁱPrinceton Plasma Physics Laboratory, PO Box 451, Princeton, NJ 08543-0451, USA

^jÉcole Nationale Supérieure de Physique, Électronique et Matériaux (Phelma), Institut polytechnique de Grenoble Alpes, Grenoble, France

* See the author list of "X. Litaudon *et al* 2017 *Nucl. Fusion* 57 102001"

E-mail: d.iglesias.fusion@gmail.com

December 2018

Abstract. The JET outboard divertor targets are the in-vessel components which receive the largest heat flux density. Surface delamination, radial cracks, and tie rod failures have been observed in the outboard tungsten-coated CFC tiles, while bulk tungsten special lamellas were intentionally melted in dedicated experiments. These different types of damage were not reproducible using existing models and tools. Several analysis and development activities have been completed during the last campaigns for improving the tools used for prediction of the plasma parallel heat flux density and the thermo-mechanical behaviour of the tiles. Experimental thermography measurements at different impinging angles, interpreted with new algorithms including a correction to the optical projection have led to a reduction of the peak parallel heat flux density of 1/3 compared to the previously estimated value. Integrity assessments are performed using the engineering footprint concept, which averages ELM and inter-ELM plasma load. Improvements on the ELM profiles result in a fall-off length for this engineering footprint of one order of magnitude larger than that inferred from the inter-ELM scaling laws. All these advances have been implemented in integrated analysis tools which can quickly predict the behaviour of the divertor tiles in an automated and power consistent manner. This development carried out at JET supports the experimental understanding, enhances the real-time protection systems, improves the evaluation of the operating instructions, and is also transferable to ITER.

1. Introduction

The assumption that λ_q from the well-known inter-ELM scaling laws [1] applies for the heat flux on all components leads to an overestimation of the peak temperature and unnecessary limitations in total power or energy. The ELMs produce an effective spread of the averaged power at the divertor surfaces which may also be estimated as a machine-specific function depending on several plasma parameters [2]. On the other hand, if this broader power deposition profile is not considered, observed damages on components assumed to be sheltered cannot be predicted.

On JET, the damage to the divertor is prevented by a set of Operating Instructions [3], which limit the energy and maximum surface temperature and are enforced during pulse preparation. Maximum temperature limits depend on the tiles material. Bulk tungsten is used for the four stacks (A-D) of tile 5, while the rest of tiles are made of W-coated CFC (see Fig. 1). IR protection camera real-time measurements ensure these limits are imposed during each discharge. Even with these measures in place, several damaged tiles were found during the last two shutdowns (Fig. 2 central and right). In the case of tile 6, three new tiles needed to be installed due to tie rods failures, while another six tiles were replaced due to cracks appearing in its central sections at different locations.

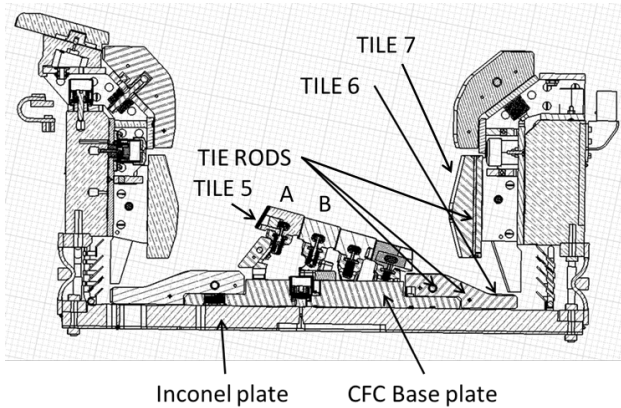


Figure 1. Section of the JET divertor with the centre of the machine to the left of the image, showing the complex assembly of the bulk tungsten tile 5, and the other outer target highest loaded W-coated CFC tiles 6 and 7.

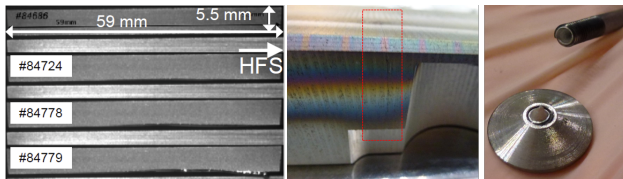


Figure 2. Failures characterized at the divertor targets: evolution of a protruding edge lamella during the 2013 W-melting experiments (left), cracks detected at the central sections of tile 6 (centre), and broken tie-rods (right).

The surface delamination and radial cracks observed in the outboard tungsten-coated CFC tiles were not reproducible using existing models and tools. Tie-rod failures were analysed using a simplified triangular heat flux, as their behaviour is more dependent on the total energy absorbed by the tile and the strike-point (SP) location, and less on the actual shape of the footprint. This is due to the high diffusivity of the CFC and the distance of the tie rods to the plasma facing surface. The same simplification cannot be applied to other damage mechanisms such as overheating or surface cracking, as these effects are far more sensitive to the shape of the heat flux density applied at the tiles surface. In any case, an estimation for the amplitude, width, and projection of the parallel heat flux was lacking for defining the shape of the surface heat flux even if simplified including inter-ELM and ELM effects.

In addition, at the ITER organization's request, dedicated experiments at JET studied the impact of melting an exposed tungsten edge [4] (Fig. 2 left). Interpreting these experiments required the application of unexplained mitigation factors for matching the IR derived parallel heat flux profiles to those derived from thermal simulations [5]. The unexplained mitigation factors were solved first for the L-mode case by adjusting a constant footprint for matching the simulations to the experimental measurements [6], and later for the H-mode discharges by using a time and space variable loading model characterized processing experimental thermography measurements [8]. These new interpretations of the melting experiment results were possible thanks to a new design of the experiment featuring a 15 sloped lamella, along with the development of new tools for increased accuracy calculating inter-ELM and L-mode footprints in irregular geometries, ELM transient loads, and heat flux in shadowed areas. As a result, the parallel heat flux at the outboard targets of the JET divertor was fully characterized at different power levels.

The paper presents an improved characterisation of the parallel heat flux at the divertor, complemented by the definition of the engineering footprint profile. Both advances have been implemented in an integrated assessment procedure for understanding and preventing damage at the outer divertor tiles in preparation for the upcoming high-power JET campaigns.

2. Modelling advances

The parallel heat flux density at the divertor is reconstructed from the surface temperature measurements acquired by the experimental IR camera using inverse analysis techniques. The new code ALICIA [7] has been developed for a realistic representation of the tile geometry and coating thickness leading to an improved calculation of both the surface heat flux density and energy. A set of geometrical and loading projection corrections have been introduced which lead

to an overall reduction of the measured parallel heat flux density. The time-averaged footprint is characterized at the equatorial plane and fitted to plasma operation parameters.

2.1. Parallel heat flux experimental measurement

The change from carbon to the all-metal ITER-like wall has motivated the development of new inverse analysis tools for analysing the coated CFC and bulk tungsten tiles where thin graphite layers are not found. For the calculation of the heat flux at the ILW divertor it is critical to match their complex surface and body geometry. The poloidal profile can now be represented by a finite element (FE) 2D mesh, while the toroidal irregularities may be included by the consideration of two geometrical factors [8]. Non-standard lamellas were installed in dedicated experiments for studying the melting events at the JET bulk-W tile 5. The outer SOL plasma impinged these special geometries at angles varying from 2 to 90, allowing to separate the optical projection of the parallel heat flux from a non-parallel component which was found to be 20% of the surface heat in L-mode and 30% in H-mode for the standard tiles. These contributions correspond to 1.2% and 1.9% of the parallel heat flux density, respectively. The quantification of the non-parallel components was confirmed by the measurements performed at a shadowed lamella at the same toroidal location.

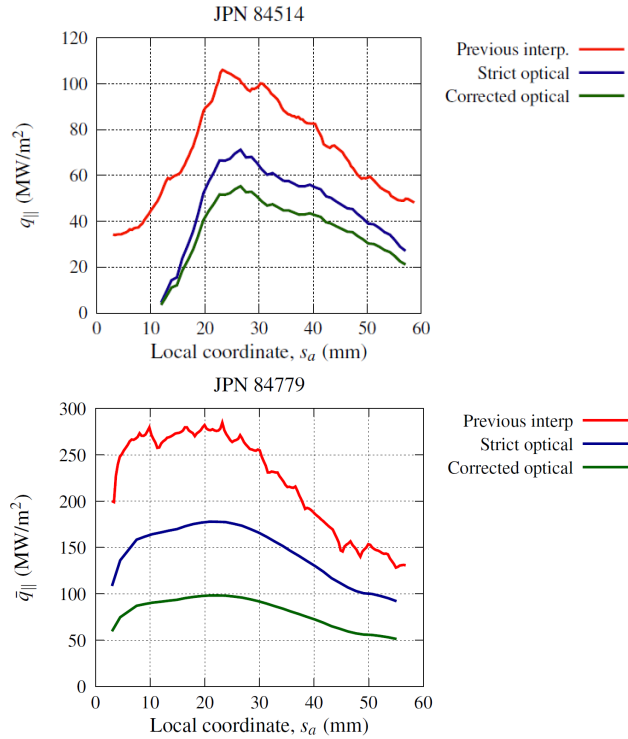


Figure 3. Parallel heat flux density reconstruction at the outer divertor bulk-W tiles for L-mode (left) and H-mode (right) discharges: IR derived profiles (red) at the tile surface, with geometrical (blue), and projection (green) corrections [8].

All these improvements new FE inverse code, 3D geometric parameters, and non-parallel heat flux contribution-shave major impact on the experimental measurement of the parallel heat flux. the resulting corrected optical projection shows a reduction of the parallel heat flux density of 50% for L-mode and 60% for H-mode (see Fig. 3) compared to previous estimations [8].

2.2. Engineering footprint characterisation

The measured SOL heat flux density profile has been characterized at the equatorial plane by an engineering footprint [2], calculated using time-varying plasma parameters fitting a Gaussian distribution convoluted with an exponential function [1]. The IR derived heat flux at the divertor targets (bulk-W and W-coated CFC tiles) is averaged over 0.1 seconds, including ELM and inter-ELM contributions, and then projected to the equatorial plane using the equilibrium calculated using EFIT. Five parameters were chosen for fitting both the decay length, λ_q , and the standard deviation of the Gaussian, S .

Several shots were analysed at tile 5 for both the flat C-wall and ILW bulk-W lamella arrangement [2]. For the latter, the profile was fitted using either one or two stacks with ~ 60 mm length each. No satisfactory results were achieved using more than one stack due to issues in the IR derived data from the second stack, which might be due to diagnostic errors derived from reflections. The spread of the statistical analysis (Fig. 4 upper) is similar for all cases once the ILW 2 stacks data points are discarded.

During the last JET campaign, a tile 6 extension was installed allowing IR measurements of its surface temperatures. Few fixed strike point shots were available for making a similar analysis with all of them leading to values much larger for λ_q and S (Fig. 4 lower), clearly showing a different scaling at this corner tile which has a stronger instability regarding the position of the footprint.

The fit uses the following expressions with independent coefficients for plasma current and toroidal field. The other three indices depend on the plasma equilibrium and have different values for each tile (see Table 1).

$$\lambda_{footprint} [mm] = \min(1.6 \cdot I_p^{-0.024} B_t^{0.52} n_e^{c_\lambda} P_{SOL}^{d_\lambda} f_{ELM}^{e_\lambda} + 0.006\sigma_{RF}, 0.02) \quad (1)$$

$$S_{footprint} [mm] = \min(1 \cdot I_p^{0.74} B_t^{-0.83} n_e^S P_{SOL}^{d_S} f_{ELM}^{e_S} + 0.002\sigma_{RF}, 0.02) \quad (2)$$

With:

I_p : Plasma current in MA,

B_t : Toroidal magnetic field in T,

n_e : Line integrated electron density $10^{20} m^{-2}$,

P_{SOL} : Power in the scrape-off layer (SOL) in MW,

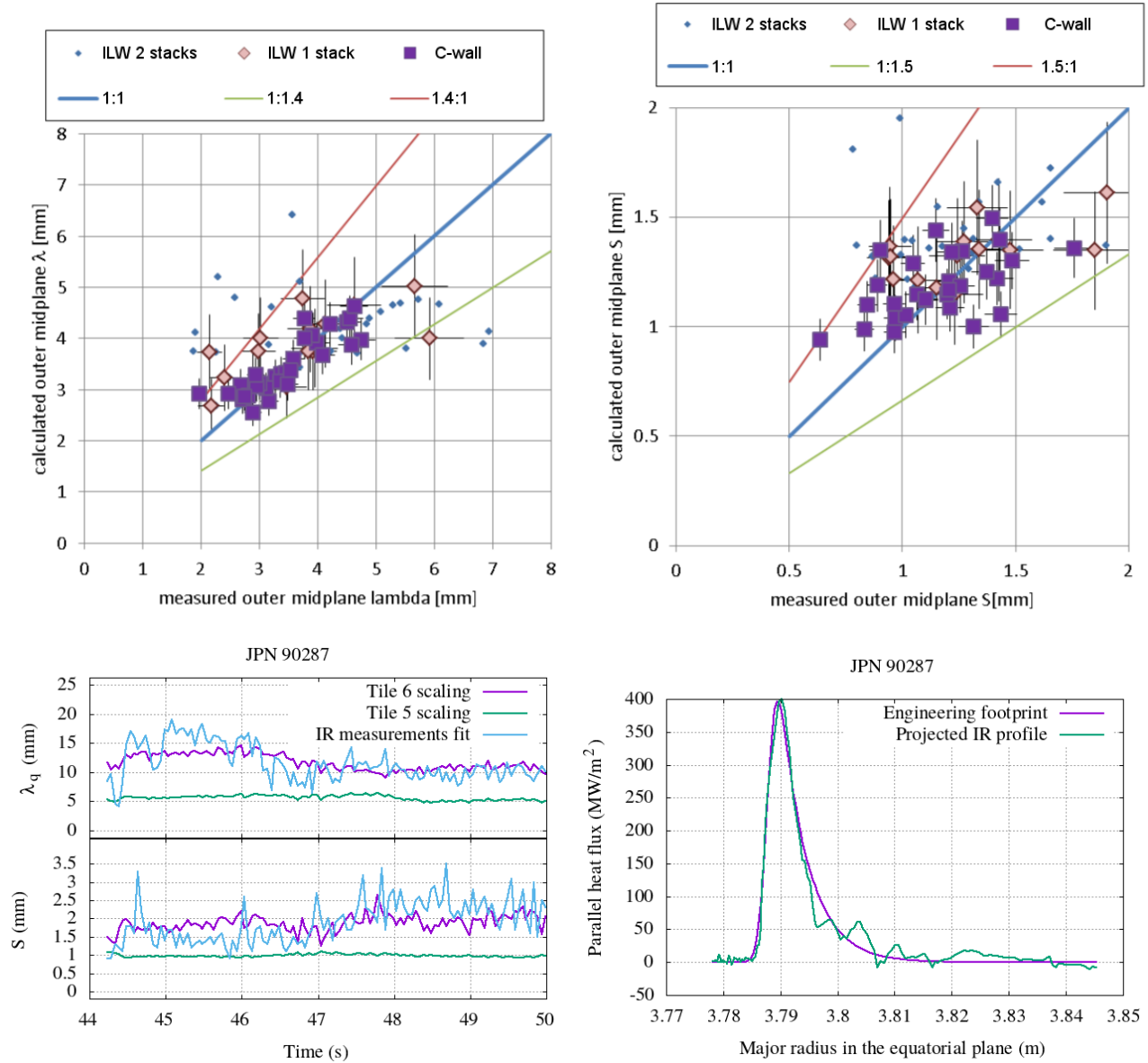


Figure 4. Engineering footprint computed at the equatorial plane: comparison between estimated and measured parameters at tile 5, with ILW 1-stack and C-wall being used for the correlation (upper [2]), time-evolution of tile 5 and 6 scaling compared with the IR fit from tile 6 during fixed strike point discharge JPN 90287 (lower left), and typical fit (purple) of the fully corrected IR (green) profile (lower right).

f_{ELM} : ELMs frequency in Hz,

σ_{RF} : Standard deviation of the radial field circuit current in A, and

c, d, e are coefficients dependent on the tile in study, as shown in table 1.

3. Divertor integrity predictive analysis

The improvements in the reconstruction of the plasma heat flux density at the divertor targets have been implemented into three different workflows, depending on the objective of the analysis:

Table 1. Fitted parameters for the engineering footprint at outboard divertor tiles 5 and 6

Tile # / Parameter	c	d	e
Tile 5 / $\lambda_{footprint}$	-1.00	0.023	0.15
Tile 6 / $\lambda_{footprint}$	0.45	0.40	0.20
Tile 5 / S	-0.6	0.052	-0.11
Tile 6 / S	0.01	-0.077	0.54

- JET Operating Instructions checks can be performed running synthetic shots in the integrated modelling tool VITA [7] for calculating expected temperatures

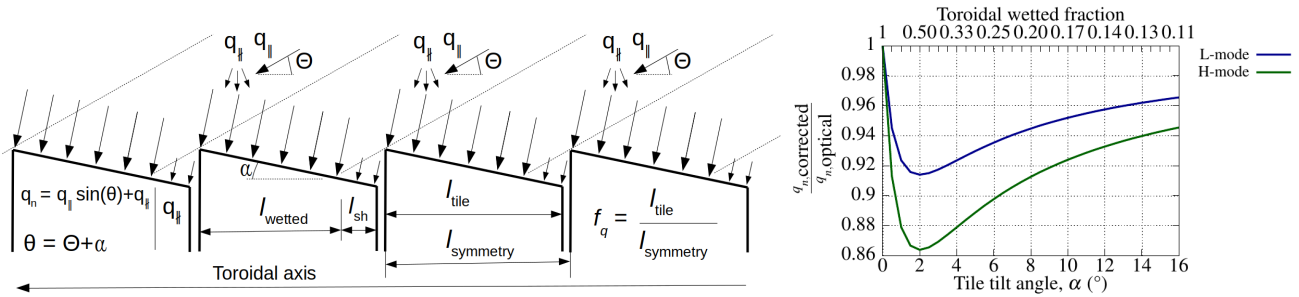


Figure 5. Toroidal section for the SOL heat flux projection model used for predictive analysis (left), and ratio between corrected and strict optical projections (right) for a typical magnetic angle of $\Theta = 2$.

and tile energy.

- Real-time protection using WALLS [9] is improved by a better estimate of the heat flux profiles using the engineering footprint correlations, and by fast FE 2D models delivering accurate temperatures.
- Post-pulse checks are now possible even if the protection or experimental cameras is not available during the shot. For this, VITA connects to the JET database for reading the stored signals which allow the calculation of the SOL heat flux density at the equatorial plane and its projection on the tiles of interest. The surface load is then linked to 3D FE codes, such as ANSYS, for performing transient thermo-mechanical assessments.

3.1. Validation activities

The surface heat profile at the divertor is calculated using magnetic projection of the parallel heat flux in 2D using EFIT, or in 3D using SMARDDA [10] plus an additional non-parallel component with the projection scheme shown in Fig. 5 left. The total power at the shadowed regions increases with the toroidal wetting factor (TWF), reducing the maximum surface heat flux between $\sim 5\%$ for L-mode and $\sim 10\%$ for H-mode for typical JET TWF values (Fig. 5 right).

The characterisation of the engineering footprint using fixed strike point discharges has proven reliable when simulating the behaviour of the tiles for both fixed and swept strike point shots. The latter are now the main mitigation strategy for reducing the surface temperatures at the tiles for high power and high energy discharges [11]. Fig. 6 (left) shows how the maximum temperature evolution is matched to the IR experimental data for two swept shots. The response is not only mimicked during the flat top stage but also during the cooldown, as a result of the correct estimation of the amount of energy going into the tile. When systematically run over a set of well diagnosed Hybrid scenario discharges [12], the error obtained for the peak temperature at the surface is $\pm 15\%$ (Fig. 6 right).

As detailed in table 2, in comparison with the worst-case given by the λ_q scaling laws [1], the engineering

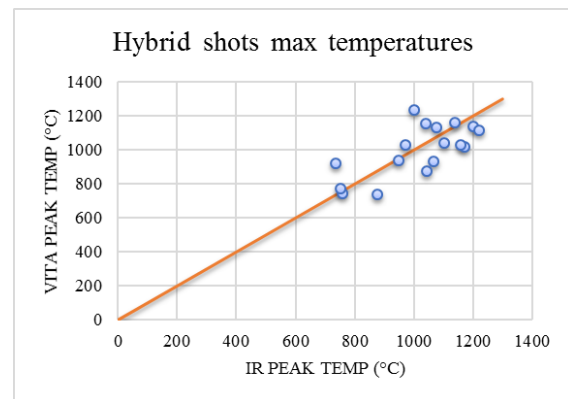
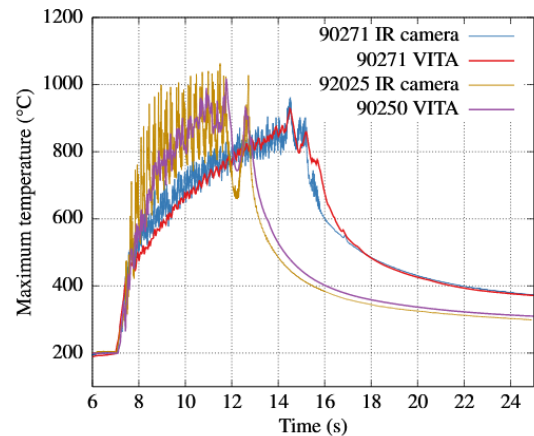


Figure 6. Simulation of thermal effects for swept strike point discharges: prediction of transient temperature evolution using VITA (upper [7]) and comparison between peak temperatures and IR measurements for several hybrid scenario discharges (lower).

footprint always leads to a broader profile [2]. The broadening produced by ELM strikes and natural strike point movements of the plasma depends on the magnetic equilibrium and therefore is different for each tile: varying from 50% increment of the footprint width for tile 5, and up to 5 to 10 times wider for tile 6 which is consequently used for high performance JET discharges.

Table 2. Comparison between fall-off lengths and engineering footprint widths at different tiles for similar Hybrid shots.

shot	λ_q inter-ELM	$\lambda_{footprint}$ T5	$\lambda_{footprint}$ T6
90271	2.1	2.2-3.5	9-17
92025	2.1	2.1-3.0	11-19
92436	2.1	2.1-2.5	10-19
92398	2.5	2.0-3.2	13-16

3.2. Application to predictive integrity assessments

Two alternative procedures may be followed for recreating the different damages observed at the divertor tiles. The use of IR derived heat flux is useful for reconstructing the parallel heat flux at a reference surface and then project it to a misaligned tile [7], while alternatively, the engineering footprint may be used for predicting and avoiding failures before running a discharge [13]. The deformation and internal stress distribution of tile 6 (Fig. 7 right) was compared using the heat flux derived from IR measurements with a fully synthetic approach without using any thermography data, obtaining a consistent error of $\sim 20\%$ on the safety side.

The modelling activities have allowed identifying the origin of the cracks and tie-rod failures. The former is due to the differential expansion between the heated and shadowed areas of the tile surface and facilitated by the low resistance of the CFC in the toroidal direction, being this perpendicular of the CFC plies. The latter depends purely on the expansion and bending of the whole tile. Both failure modes have been found to be very much dependent on the energy deposited into the tile during the discharge and the location of the strike point position (Fig. 8). By running synthetic shots for the levels of power and duration required for the upcoming DT campaign, it has been concluded that the crack failures are likely to occur although their impact to operations is minimal if the tie-rods do not fail. Sensitivity analysis has shown that the location of the cracks may be limited by shifting the outboard strike point towards the low-field side of the tile [13].

The integrity of the tile is ensured only if the tie-rods are well protected. Conservative fatigue limits based on experimental evidence have been set for avoiding their failure. The accumulative damage in the future will be monitored by energy accounting for low energy discharges, while the assessment of high energy discharges may be more accurately performed running the full 3D simulation, including the effect of the strike point location and footprint shape. The integrated workflow developed for this assessment linking VITA and ANSYS allows to complete the full study in less than 10 minutes, which is less than the time between JET discharges.

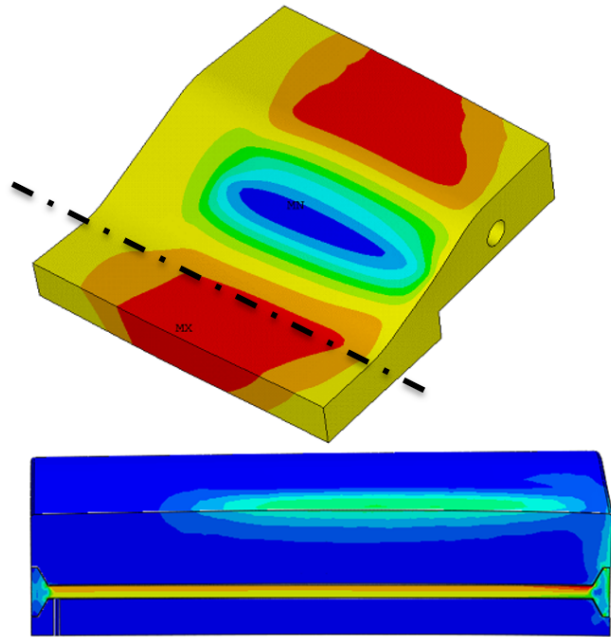


Figure 7. Simulation of thermo-mechanical effects: temperature [C] distribution predicting melting events in misaligned surfaces using ALICIA and ANSYS (left [8]), and toroidal stress [Pa] distribution prediction linking VITA to ANSYS (right [13]), with areas in red matching observed CFC crack damage locations.

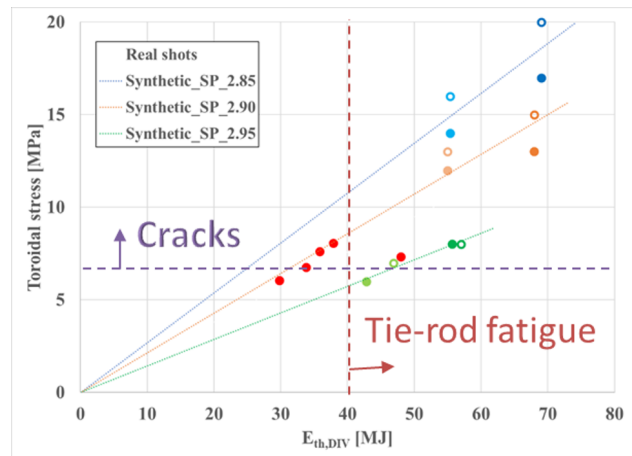


Figure 8. Synthetic discharges with 33 MW and 40 MW input power and 6 seconds flat-top, strike point at different radial positions (in meters with respect to the centre of the machine) and sweeping amplitudes of 3mm (hollow) and 6mm (filled). Comparison with real shots simulations [13].

4. Summary and conclusions

The definition of a predictive model requires a reliable estimation of the average normal heat flux at different divertor tiles as a function of input power, magnetic equilibrium, and basic plasma parameters. This has been developed in three steps: improving the calculation of the normal heat flux by fast IR thermography, quantifying the heat flux density contributions on the exposed and

shadowed surfaces, and finally, fitting its time average to five different operational parameters. The thermo-mechanical response of the divertor tiles to this predicted load has been validated to experimental data and then used for determining the risk of failure of upcoming high-power campaigns. The engineering footprint is machine specific as it includes ELMs and strike point movements due to a mix of plasma current transients and control system response [8]. Nevertheless, the approach developed at JET can be performed in the future in ITER using early low power H-mode shots to characterize its particular engineering footprint.

The validated approach can now be used for the preparation of JET operations. Before a discharge, automated predictive analysis may be run for ensuring that the maximum temperature and stress levels remain within allowable limits. The SOL parallel heat profiles are calculated in the equatorial plane and then projected to the divertor geometry either using a simple 2D projection for a quick solution, or with the more involved 3D line-tracing SMARDDA software [10]. In JET, the engineering footprint may lead to a 5 to 10 times wider footprint compared to that obtained using typical inter-ELM scaling laws, highly increasing the divertor operational envelope. The observed failure modes may currently be reproduced and therefore avoided by means of coupled-field 3D thermo-mechanical models. The error between measurements and modelling regarding energy and sustained temperatures is typically $\sim 15\%$.

All these improvements have been implemented in integrated analysis tools. The thermal behaviour is calculated in a matter of seconds while a 3D thermo-mechanical assessment can be automatically performed in less than 10 minutes. This development carried out at JET supports the experimental understanding, enhances the real-time protection systems, improves the evaluation of the operating instructions, and is also transferable to ITER.

Acknowledgements

This work has been carried out within the framework of the EUROfusion Consortium and has received funding from the Euratom research and training programme 2014-2018 under grant agreement No 633053. The views and opinions expressed herein do not necessarily reflect those of the European Commission or of the ITER Organization.

References

- [1] Eich T. *et al* 2013 Nucl. Fusion **53**:9 093031.
- [2] Riccardo V. *et al*, Power footprint definition for JET divertor protection, 22nd PSI, Roma, Italy (2016).
- [3] Riccardo V. *et al* 2009 Phys. Scr. **T138** 014033.
- [4] Coenen J.W. *et al* 2015 Nucl. Fusion **55** 023010.
- [5] Arnoux G. *et al* 2015 J. Nucl. Mater. **415-419** 463.
- [6] Corre Y. *et al* 2017 Nucl. Fusion **57** 066009.
- [7] Iglesias D. *et al* 2018 Nucl. Fusion **58** 106034.

- [8] Iglesias D. *et al* 2017 Fusion Eng. Des. **145** 71–76.
- [9] Valcarcel D. *et al* 2013 Fusion Eng. Des. **89**:3 243–258
- [10] Arter W. *et al* 2014 IEEE Trans. Plasma Sci. **42**:7 1932–1942
- [11] Silburn S. A. *et al* 2017 Phys. Scr. **T170** 014040.
- [12] Joffrin E. *et al* 2005 Nucl. Fusion **45** 626.
- [13] Richiusa M. L. *et al*, Maximizing JET divertor mechanical performance for the upcoming Deuterium-Tritium experiments, Fusion Eng. Des. (2018) Submitted.